Supporting Information

Anomalous Increase of Dielectric Permittivity in Sr-doped CCTO Ceramics $Ca_{1-x}Sr_xCu_3Ti_4O_{12}$ ($0 \leq x \leq 0.2$)

Rainer Schmidt*,†,‡ and Derek C. Sinclair‡

† Universidad Complutense de Madrid, Departamento Fisica Aplicada III, GFMC, Facultad de Ciencias Fisicas, Madrid 28040, Spain

‡ The University of Sheffield, Engineering Materials, Sir Robert Hadfield Building, Mappin Street, Sheffield S1 3JD, United Kingdom

* Corresponding author. Email: rainerxschmidt@googlemail.com

Part I.) Phase Analysis

Part II.) Impedance spectroscopy data analysis

I.) Phase Analysis

Figure S1 shows X-ray diffraction (XRD) patterns of $Ca_{1-x}Sr_xCu_3Ti_4O_{12}$ (CSCTO) powders for x = 0.2, prepared at 1000 and 1100 ºC, and for x = 0.4 prepared at 1000 ºC. The x = 0.2 powder was single-phase after heat treatment at 1000 ºC and is iso-structural with un-doped $CaCu_3Ti_4O_{12}$, whereas the corresponding powder of x = 0.4 contained $SrTiO_3$ and TiO_2 as additional phases.

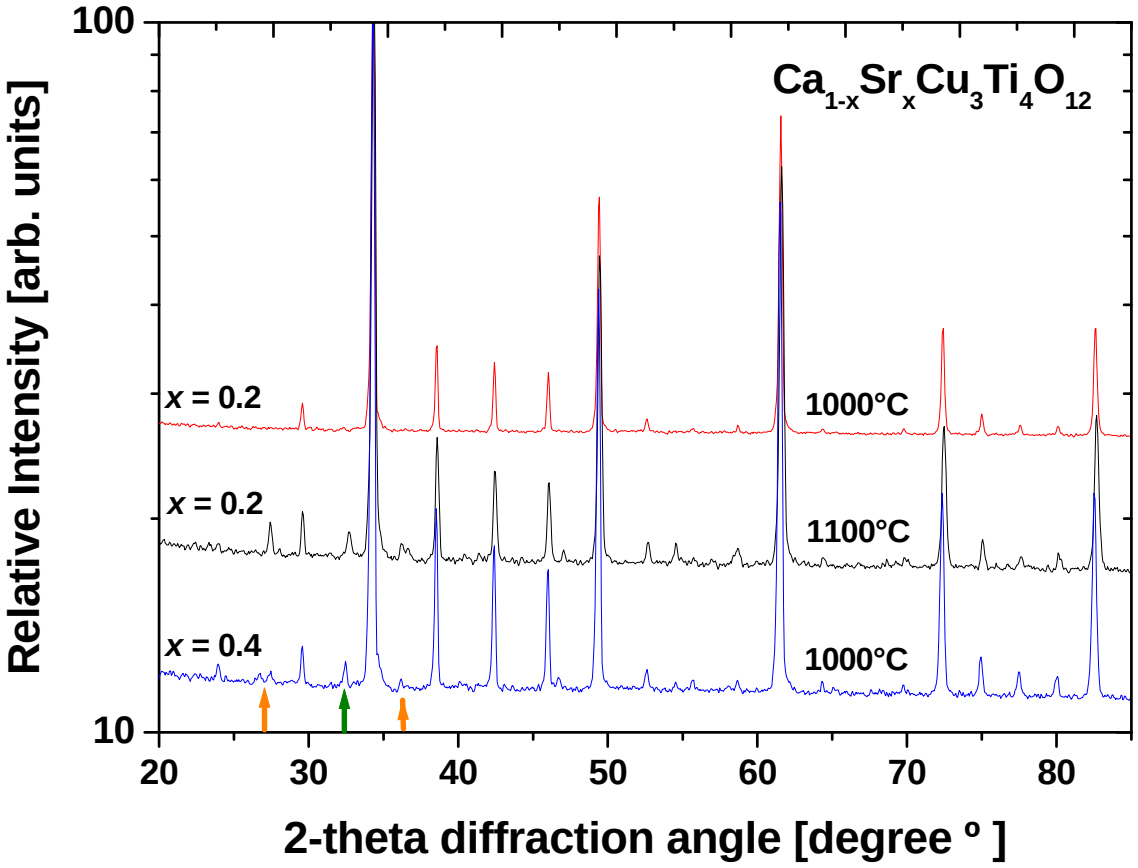

Figure S1 XRD patterns for $Ca_{1-x}Sr_xCu_3Ti_4O_{12}$ powders x = 0.2 and 0.4 prepared at 1000 ºC and for x = 0.2 prepared at 1100 ºC. Secondary phases are indicated by arrows: green arrow for $SrTiO_3$ and orange arrows for TiO_2.

After heat treatment at 1100 ºC neither powder was single phase; both contained $SrTiO_3$ and TiO_2 as additional phases. These results confirm that the solid solution limit has been exceeded in the x = 0.4 sample and that a maximum heat treatment temperature of 1000 ºC is the limit to obtain single-phase powders within the solid solution. Pellets of composition x = 0.2 and 0.25 were sintered at 1000 ºC and further investigated using scanning electron microscopy (SEM) operating in secondary electron and backscattered electron modes. Figure S2 shows a comparison of the two operating modes used on the same sample area for x = 0.2 and 0.25.

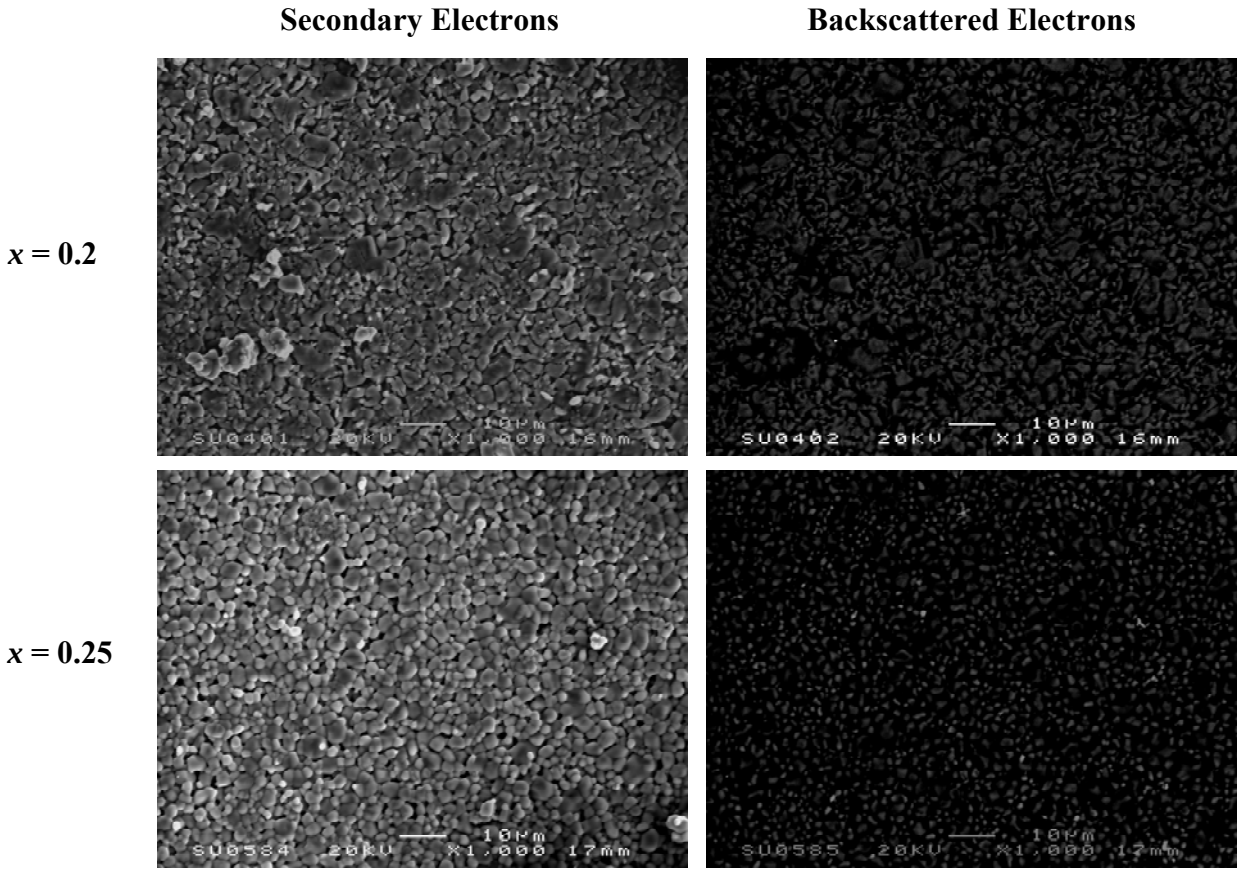

Figure S2 SEM images taken in secondary electron and backscattered modes for 1000 ºC sintered pellets of composition x = 0.2 and 0.25.

No elemental contrast is obvious in the backscattered image for $x = 0.2$, which is a strong indication for the absence of any impurity phase. In contrast, a small amount of bright $SrTiO_3$ spots is visible in the backscattered image for $x = 0.25$, indicating the solid solution limit has been exceeded. The small volume fraction of $SrTiO_3$ secondary phase particles in $x = 0.25$ is below the detection limit of laboratory XRD.

II.) Impedance spectroscopy data analysis

In the main body of the text we have proposed that the value of the high-frequency and low-capacitance plateau (C1*) in spectroscopic plots of the real part of capacitance (*C*') can be used as an estimate for the intrinsic bulk capacitance (see Figures 2a & b in the main text). It can be shown that C1* formally contains a contribution from the GB capacitance (C2) and, therefore, for precise bulk ε_r values a correction of C1* for the GB capacitance is necessary. This GB effect is based on the brick-work layer model, where ideal bulk and GB relaxations are represented by two parallel resistor-capacitor (RC) elements connected in series. Such a model is shown in Figure S3. If the GB relaxation is described by R2-C2 and the bulk by R1-C1, the value of the high-frequency and low-capacitance plateau C1* is given by:

$$C1^* = \frac{C1 \times C2}{C1 + C2}; \qquad (1)$$

Equation (1) shows that the "true" intrinsic bulk capacitance value C1 may be larger than C1*. In order to obtain C1 from C1* we have determined the GB capacitance (C2) from plots of the imaginary part of the capacitance *C*'' vs the real part *C*'. Such Cole-Cole plots (Figure S3) display an ideal semicircle in the case of two parallel RC elements connected in series for ideal GB and bulk relaxations. For Sr-doped CCTO ceramics, the GB and bulk resistance values always differ by at least 4 orders of magnitude. In this case, the low frequency *x*-axis (*C*' axis) intercept corresponds to the GB capacitance C2, whereas the high frequency intercept corresponds to C1*. The size of the semicircle increases with *x* and therefore shows an increase of GB capacitance with *x*. We have determined the GB capacitance from the low frequency *x*-axis (*C*' axis) intercept

and used equation (1) to determine C1 for each sample. C1 values varied from C1* by + 16 % for x = 0, and this deviation decreased to + 8 % for x = 0.2. The deviation is small when compared to the total increase of bulk dielectric permittivity by ~ 300 % from x = 0 to 0.2. This confirms that although C1 values are preferable, C1* is a good approximation of the bulk permittivity for these samples.

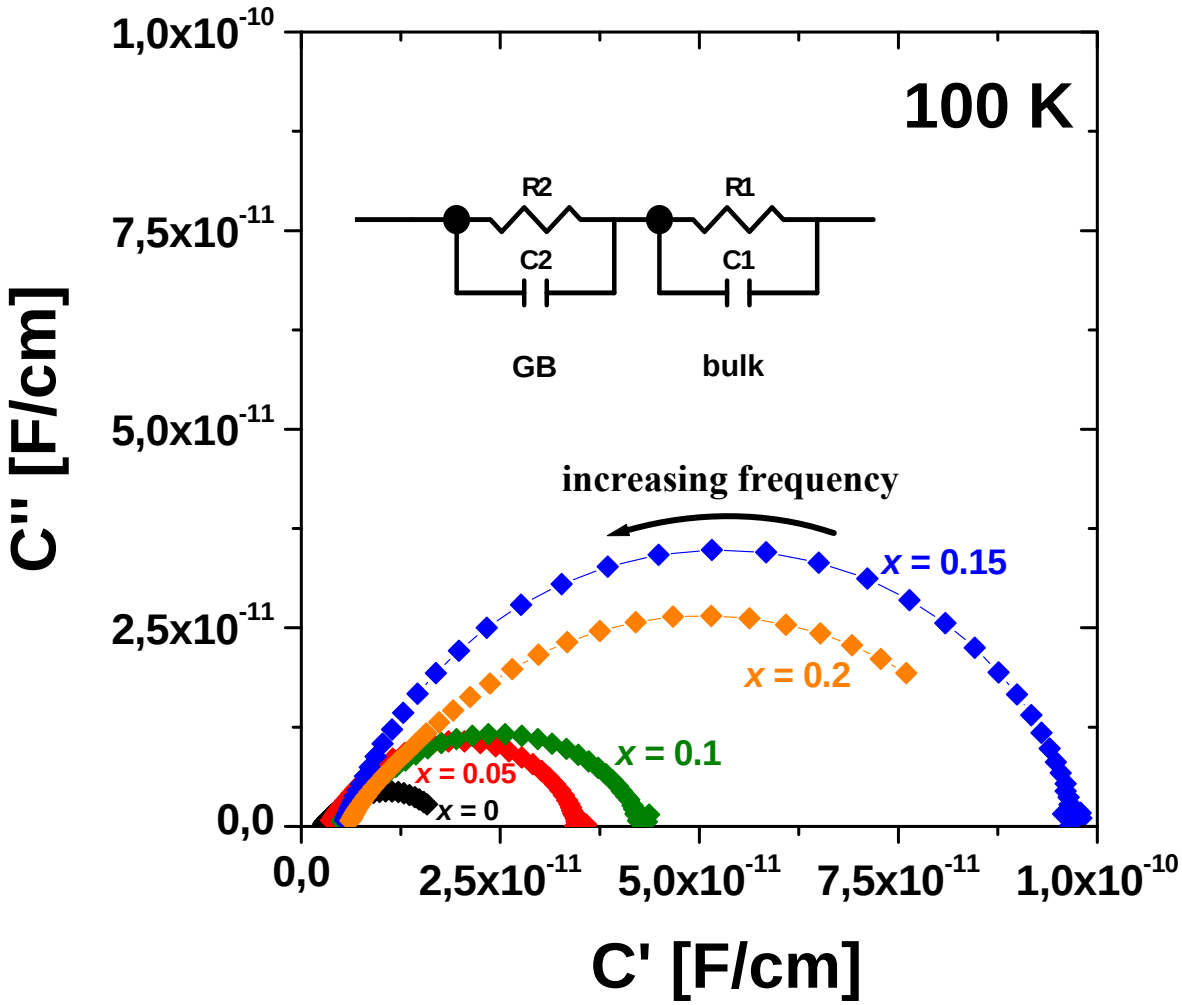

Figure S3 Cole-Cole plots of *C*'' vs *C*'. Data taken at 100 K from x = 0 to 0.2 samples. Inset: equivalent circuit model for ideal bulk and GB relaxations.

Figure S3 shows the Cole-Cole semicircles to be depressed. This is a clear sign of non-ideal relaxation processes, and our bulk capacitance correction may be regarded only as an approximation. Data for x = 0.15 in Figure S3 is an exception to this trend. The semicircle is less depressed and a more ideal relaxation process is observed.

To further investigate the trend of ε_r with x, the data at 100 K have been plotted as spectroscopic plots of the imaginary part of the dielectric modulus formalism, M''.

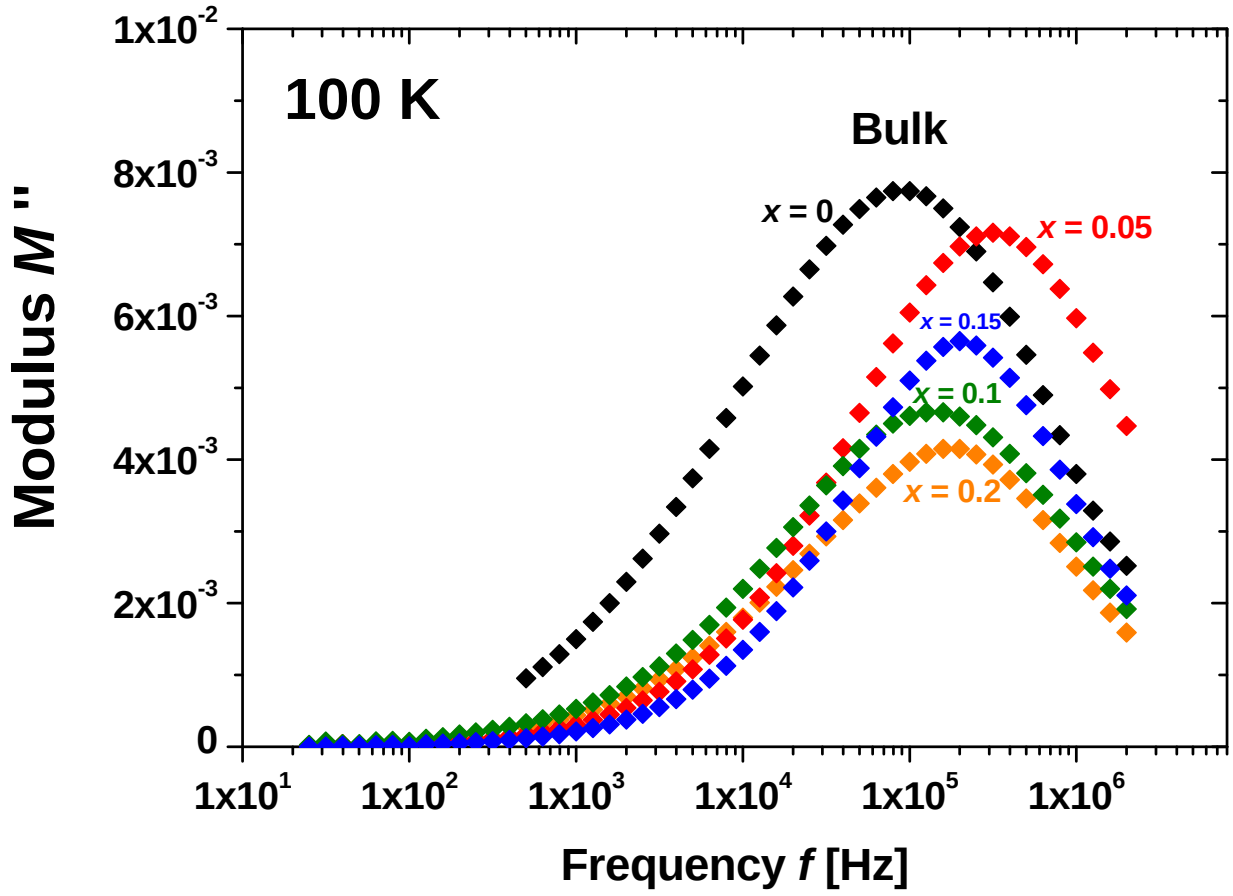

Figure S4 M'' vs frequency f; at 100 K for x = 0 to 0.2. The M'' peak is proportional to the reciprocal of the bulk capacitance.

Figure S4 displays the bulk relaxation peak for all samples at 100 K. In the framework of an ideal Debye relaxation process, as described by an ideal parallel RC element, the bulk dielectric relaxation peak in M'' vs f is expected to be a Lorentz function, where the height of the peak is proportional to the reciprocal of the bulk capacitance. Figure S4 reproduces the trend of C1 vs x shown in Figure 3 in the main text, because the peak height reduces with x. The only exception to this trend is the data for $x = 0.15$. An explanation for this is given in the following paragraph.

All curves in Figure S4 show considerable relaxation peak broadening and deviate from the ideal Debye behaviour. Relaxation peak broadening is usually associated with a non-ideal relaxation process. In such a case, the peak height is reduced to ensure the spectral weight of the peak is preserved. Figure S4 shows that the relaxation peak broadening and the concomitant peak height reduction for $x = 0.15$ is less pronounced when compared to all the other samples, thus leading to a comparatively large peak. Such limited relaxation peak broadening is signature of a more ideal relaxation and is consistent with the Cole-Cole plots (Figure S3), where $x = 0.15$ showed a more ideal response as well compared to the other samples. Furthermore, $x = 0.1$ displays a particularly broad relaxation peak and the peak height is substantially reduced. The bulk permittivity values obtained from the peak heights [$= 1/2\ M''(f_{max})$] are in a similar range to those shown in Figure 3 in the main text (on average ε_r values from $M''(f_{max})$ data are ~ 20% larger).